

Impact of a photovoltaic plant connected to the MV network on harmonic distortion: an experimental assessment

*Original*

Impact of a photovoltaic plant connected to the MV network on harmonic distortion: an experimental assessment / V., Barbu; Chicco, Gianfranco; Corona, Fabio; N., Golovanov; Spertino, Filippo. - In: SCIENTIFIC BULLETIN - "POLITEHNICA" UNIVERSITY OF BUCHAREST. SERIES C, ELECTRICAL ENGINEERING AND COMPUTER SCIENCE. - ISSN 2286-3540. - STAMPA. - 75:Issue 4(2013), pp. 179-194.

*Availability:*

This version is available at: 11583/2538720 since:

*Publisher:*

"POLITEHNICA" UNIVERSITY OF BUCHAREST

*Published*

DOI:

*Terms of use:*

openAccess

This article is made available under terms and conditions as specified in the corresponding bibliographic description in the repository

*Publisher copyright*

(Article begins on next page)

## IMPACT OF A PHOTOVOLTAIC PLANT CONNECTED TO THE MV NETWORK ON HARMONIC DISTORTION: AN EXPERIMENTAL ASSESSMENT

Valentina BARBU<sup>1</sup>, Gianfranco CHICCO<sup>2</sup>, Fabio CORONA<sup>3</sup>, Nicolae GOLOVANOV<sup>4</sup>, Filippo SPERTINO<sup>5</sup>

*This paper deals with the analysis of the experimental results obtained on a photovoltaic system composed of a number of inverters connected to the point of common coupling. The data have been gathered from the field for a period of one week through a network analyzer. The harmonic distortion of phase voltages and currents has been characterized both with reference to the generation level and by taking into account statistical information (the RMS values corresponding to 90% non-exceeding probability for a given range of generation level). The results show that in the case analyzed the presence of the PV system can be beneficial to reduce the harmonic distortion of the phase voltages with respect to the distortion occurring when the PV system is not connected.*

**Keywords:** renewable energy, photovoltaic system, generation level, harmonic distortion

### 1. Introduction

In the last two decades, the increasing concerns about environmental issues, mainly air pollution, led to an increasing diffusion of renewable energy sources and to continuous improvement in the technology of electrical installations to deliver renewable energy to the grid. In this context, photovoltaic (PV) systems have been one of the most developed solutions, being attractive from the political and commercial points of view.

In the year 2011 the new PV production installed worldwide has been as high as about 30 GW, with a growth of 74% with respect to the previous year, reaching a total installed capacity of about 70 GW [1]. Several feed-in tariffs are

---

<sup>1</sup> PhD student, Faculty of Energetics, University POLITEHNICA of Bucharest, Romania, e-mail: barbuvalentina@yahoo.com

<sup>2</sup> Prof., Politecnico di Torino, Energy Department, corso Duca degli Abruzzi 24, 10129 Torino, Italy, e-mail gianfranco.chicco@polito.it.

<sup>3</sup> Politecnico di Torino, Energy Department, corso Duca degli Abruzzi 24, 10129 Torino, Italy, e-mail: fabio.corona@polito.it

<sup>4</sup> Prof., Faculty of Energetics, University POLITEHNICA of Bucharest, Romania, e-mail: nicolae\_golovanov@yahoo.com

<sup>5</sup> Politecnico di Torino, Energy Department, corso Duca degli Abruzzi 24, 10129 Torino, Italy, E-mail: filippo.spertino@polito.it

now available for PV systems, thus the maximization of the productivity is very important. This goal can be achieved by solar cell technologies with high efficiency, sun-tracking systems, proper cooling techniques for PV modules in building integrated applications, master-slave control for the inverters in large grid-connected PV plants [2]. The growth of the PV production, as well as of the production from other solutions such as wind systems, has reached a level that could significantly affect the behaviour of the electrical grid. For instance, in the occurrence of a disturbance in the electrical grid, the practice indicated by the early standards on distributed generation and resources [3]–[6], was to switch the local generation off in a short time (1s). However, with the growth of the local generation, the fast shutdown of a significant portion of local generation could cause transient phenomena in the network, increasing the risk of grid instability. In order to overcome this problem, recent standards [7]–[9] established that under certain voltage and frequency variations the local generation has to remain connected to the grid. In normal conditions, the PV system operation is affected by the uncertainty of the solar irradiance, temperature and local phenomena such as solar cells shading due to the location of the solar arrays and to passing clouds [10]. In these conditions, the main aspects refer to power quality [11]–[13]. The overall waveform quality depends on the nature of the generated power and on the structure and control of the converters that connect the PV systems to the grid [14]. In particular, in conditions of low irradiance, the waveform of the current injected in the grid becomes heavily distorted, anyway this high distortion is associated to relatively low values of the injected current and as such it does not cause particular problems for the individual installation [15]. The growth of the installed power in PV applications has led to solutions in which a number of converters are connected with respect to the point of common coupling [11][16][17] with different topologies. In the presence of multiple converters connected to the grid in a scattered way, the interaction among these converters raises the issue of how the individual contributions affect the voltage waveform in the grid [15].

This paper deals with some power quality aspects referring to a grid-connected PV plant with multiple inverters. The results obtained from monitoring the PV plant over one week are presented and discussed, highlighting the main power quality aspects. The paper is structured as follows. Section 2 shows the characteristics of the PV system analysed and illustrates the aspects referring to data logging, measurement and data management. Section 3 shows and discusses the experimental results obtained for the PV system analysed. Section 4 contains the conclusions.

## 2. Characteristics of the PV system and of the measurement system

### 2.1. PV system layout

Fig. 1 shows the layout of the PV system connected to the grid. The rated or nominal power of the PV system is  $P_n = 834.5$  kW, obtained by considering two sections with rated power values 778.61 kW and 55.89 kW, respectively. The first section concerns the most of PV arrays placed on the roof-sheds which are not perfectly South oriented. The second section includes the remainder of PV arrays installed on the flat-roof portion, which have been oriented towards South. The PV modules are connected in series, forming the PV arrays that are in turn connected in parallel to obtain a PV unit with appropriate nominal power. The PV arrays are connected to the Low Voltage grid through 8 inverters with 50 Hz transformers at the grid interface. Table 1 shows the electrical characteristics of the PV modules, while Table 2 shows the mechanical characteristics.

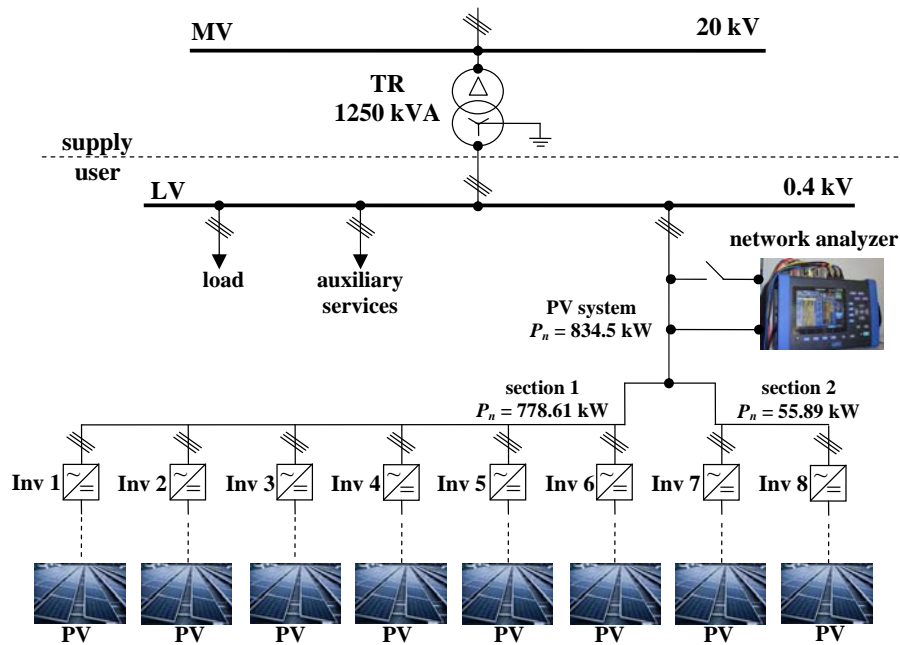


Fig. 1. Layout of the PV system connection to the Medium Voltage grid.

Table 1

Electrical characteristics of a PV module [18]

Rated power ( $P_{max}$ )*	245 W
Voltage at the maximum power point ( $V_{mpp}$ )*	30.3 V
Current at the maximum power point ( $I_{mpp}$ )*	8.09 A

Open circuit voltage ( $V_{oc}$ )		37.4 V
Short circuit current ( $I_{sc}$ )		8.61 A
PV module efficiency		15.23%
Range of operation temperatures		-40°C ... +85°C
Temperature coefficients	$P_{max}$	-0.45%/°C
	$V_{oc}$	-0.35%/°C
	$I_{sc}$	+0.06%/°C
	$NOCT$	45 ± 2°C

\* In Standard Test Conditions (STC): solar irradiance 1000 W/m<sup>2</sup>, air mass (AM) 1.5 and cell temperature 25°C.

Table 2

**Mechanical characteristics of a PV module [18]**

Type of cell	Mono-crystalline silicon ( 156 x 156 mm )
Cell connection	60 (6 x 10)
Dimensions	1638 x 982 x 40 mm
Weight	20 kg

## 2.2. Characteristics of the PV modules

The curves represented in Fig. 2, taken from the manufacturer's data [18], show that the relation between  $I_{PV}$  and  $V_{PV}$  is non-linear and depends on the level of solar irradiance on the surface of the PV panel. The maximum power point is the combination of the  $I_{PV}$  and  $V_{PV}$  values that maximize the production of the inverter, and depends both on the solar irradiance and on the PV cell temperature. In operational conditions, the optimization of the PV energy conversion is achieved through the application of a specific circuit aimed at performing Maximum Power Point Tracking (MPPT).

As it can be observed from the  $I$ - $V$  curves in Fig. 2a, the short-circuit current ( $I_{sc}$ ) changes proportionally with the solar irradiance. However, the open circuit voltage  $V_{oc}$  corresponding to the maximum power point remains almost constant at about 80%  $V_{oc}$ . This property is also used in some control circuits to create a simple control strategy aimed at making the PV system operating at the maximum power point [19]–[21]. However, this behaviour corresponds to the ideal PV system operation at clear sky. In non-ideal conditions, the maximum power point can be located at different voltages, calling for the implementation of a dedicated MPPT control circuit.

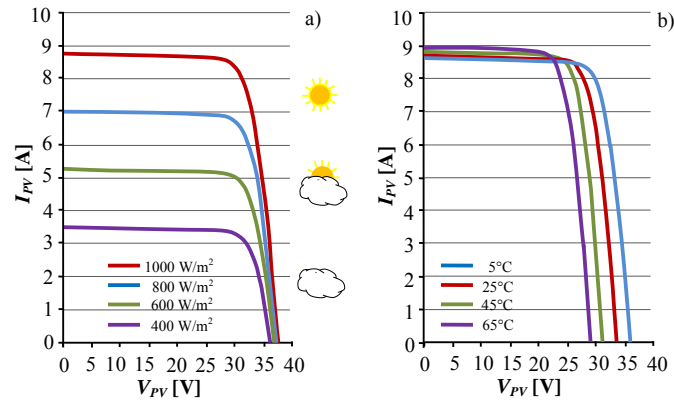


Fig. 2. Characteristics showing how the electrical current and voltage for a PV module depend on (a) the solar irradiance, and (b) the PV cell temperature for solar irradiance 1000  $W/m^2$  [18].

In Fig. 2b, the  $I-V$  curves are represented in function of different temperature values for a solar irradiance level of 1000  $W/m^2$ . In this case, the open circuit voltage  $V_{oc}$  changes in an inverse way with respect to the temperature, whereas the short-circuit current  $I_{sc}$  changes to a lower extent. In function of the effects of solar irradiance and temperature, on the  $I-V$  characteristics, the PV module manufacturers establish a set of conditions for testing the devices. In the PV industry, the standard conditions refer to the temperature of 25°C and to the solar irradiance of 1000  $W/m^2$ , as well as to air mass (AM) equal to 1.5, at null wind speed. These conditions refer to a day with clear sky and to a surface having an angle of 41.81° with respect to the horizon [22].

### 2.3. Data acquisition and viewing

The measurements have been carried out by using the high-accuracy network analyzer Hioki PW3198, during one week in July 2012. The network analyzer has eight input channels: four for voltages and four for currents through Rogowsky coils (with minimum sensitivity of 0.1 mV/A for 5000 A full scale) providing voltage signals. The instrument accuracies are for RMS voltage  $\pm 0.1\%$  of the range; for RMS current  $\pm 1.2\%$  of reading  $\pm 0.1\%$  of range with Rogowsky coils; for active power  $\pm 1.2\%$  of reading  $\pm 0.2\%$  of range with Rogowsky coils. The PW3198 provides a simultaneous digital sampling of voltage and current. The sampling frequency is 200 kHz for measurement of RMS voltage and current, active power and other power values, whereas for harmonic and interharmonic analysis the analyzer operates with 4096 points, 10 cycles (at 50 Hz) or 4096 points, 80 cycles (at 400 Hz). In normal conditions (with 16 bits of A/D converter resolution) the maximum voltage is 600 V, and in transient conditions (with A/D converter resolution 12 bits) the maximum peak voltage is 6 kV. The data

gathered can be visualized on the network analyzer viewer by choosing the variables to be shown. An example is shown in Fig. 3, with a first window on the upper part of the screen containing the list of measurements available, a successive window referring to the long-term evolution of a selected quantity in the time domain (e.g., active power), a first window on the lower side of the screen implementing a limit curve (an example is shown for the ITIC curve for voltage dip analysis) to check the effect of events, and the last window showing the voltage and current waveforms in a selected operating point or transient event.

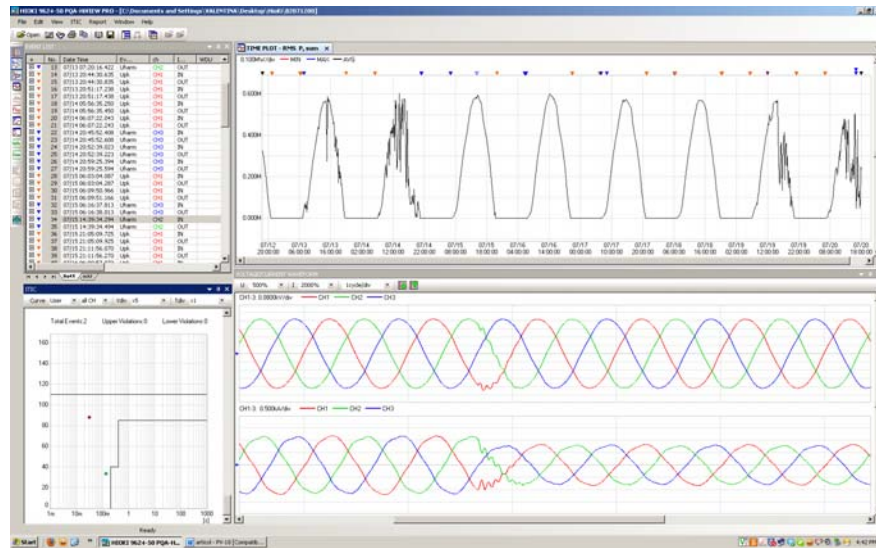


Fig. 3. The network analyzer viewer.

### 3. Experimental results

#### 3.1. Variability of the power generated by the PV system

Fig. 4 presents the variation of the active power generated by the PV system with installed power 834.5 kW, on the time span of one week. The measurements have been carried out in the location shown in Fig. 1, that is, measuring the entire generation from the PV system at the point of common coupling of the grid-connected inverters. The results show that the active power generation follows the evolution of the meteorological conditions.

Fig. 5a shows the phase voltages and Fig. 5b reports the phase currents produced in the three-phase system during the week. The voltage variations are fully acceptable, as the phase voltage oscillates in the range between 238 V and 230 V (all the values belonging to the normal conditions with RMS voltage between 90% and 110% of the rated voltage), while the current depends on the solar irradiance level.

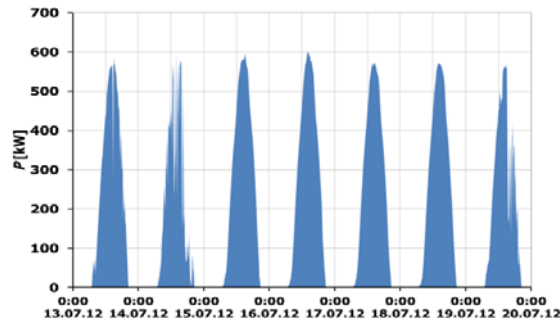
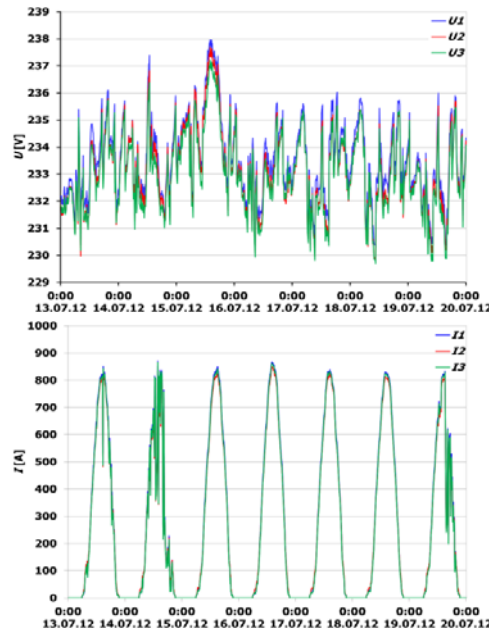


Fig. 4. Variation of the active power generated from the PV system in one week.



(a) phase voltage

(b) phase currents

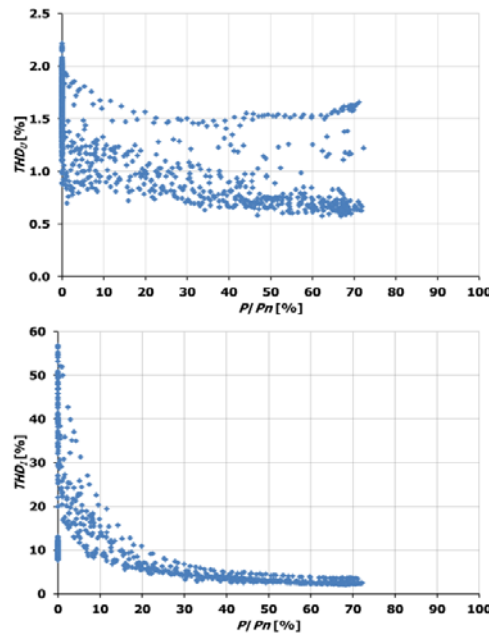
Fig. 5. Voltage and current at the point of common coupling during the week

### 3.2. Assessment of the voltage and current harmonics

The harmonics referring to the currents produced by the PV system depend on the nature of the source, as well as on the type of inverter technology used for DC/AC conversion and its control strategy. Furthermore, the output current is linked to the harmonics of the voltage at the point of common coupling, which depends on the contribution of all the generations and loads connected to the network. For the PV system, a particular aspect referring to the current harmonics is the behaviour of the inverter in conditions of reduced solar irradiance, also due to the effects of shadowing or passing clouds during the day [23].



Fig. 6 shows the total harmonic distortion  $THD_U$  of the phase voltages and  $THD_I$  of the phase currents, for different values of the *generation level*  $P/P_n$ . From Fig. 6a it is possible to conclude that the  $THD$  of the phase voltages in the system analyzed remains within acceptable ranges with respect to the limits imposed in the international standards [24]. The  $THD$  of the phase currents (Fig. 6b) becomes relatively high only when the generation level is low. For instance, when the generation level is higher than 20% the  $THD_I$  never exceeds 10%, and for generation level higher than 60% the  $THD_I$  never exceeds the limit 5% valid for rated power conditions according to [24]–[28]).

(a) phase voltage  $THD$ (b) phase current  $THD$ Fig. 6. Total harmonic distortion ( $THD$ ) of phase voltages and phase currents in one week.

Further insights on the evolution of the  $THD$  during time can be obtained by considering the behaviour of the PV system in a day with partial clouding conditions and comparing it with its behaviour in a day with clear sky. Fig. 7 shows the  $THD$  of the phase voltages. During the night, the PV system is not working and the voltage  $THD$  depends on the other components connected to the network, including the local load. During the day, the voltage  $THD$  decreases significantly. This aspect is an important confirmation of the fact that the grid connection of the PV system is able to improve the power quality characteristics at the point of common coupling, owing to the effect of the inverter control. For instance, the pulse width modulation (PWM) control moves the harmonic content

to relatively high frequencies, that may fall outside the range of frequencies detected when performing harmonic analysis (with harmonic order up to 50). A further confirmation of this fact is that, in general, the improvement in the voltage  $THD$  values is higher at clear sky with respect to the case with cloudy conditions. Hence, also during the day the voltage  $THD$  is growing when the impact of the PV system becomes lower and the system is mainly affected by the rest of the grid-connected components.

From Fig. 8, the behaviour of the  $THD$  of the phase currents during time clearly shows that cases with high values of  $THD_I$  are limited to the periods with very small solar irradiance (at the sunset and at the sunrise) and to the effects of passing clouds, while the  $THD_I$  is relatively small in conditions with relatively high solar irradiance.

The  $THD$  values provide a first indication on the impact of the PV system operation on the harmonics. However, there are two specific aspects to be considered:

1. the  $THD$  can be very high in cases with very low generation; in this case, the currents injected by the PV system in the grid could be so low to make the harmonic distortion problem practically inexistent;
2. the  $THD$  provides an overall indication on the harmonic distortion, and does not give indications on how the harmonic distortion is partitioned among the various harmonics; for this purpose, an additional detailed investigation on the individual harmonic distortion is needed.

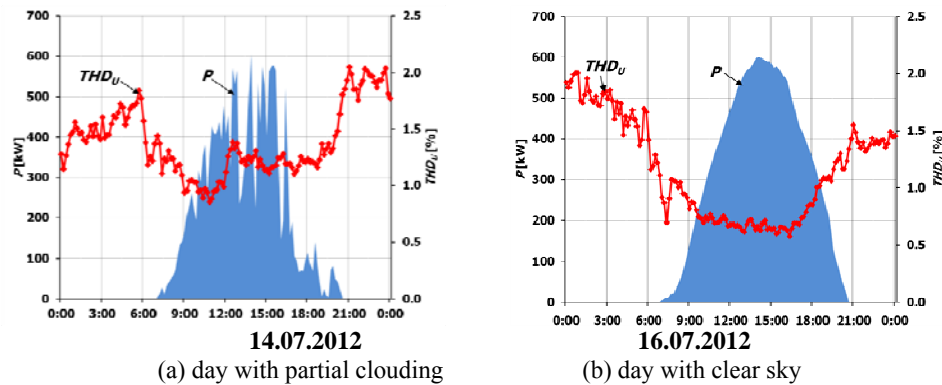


Fig. 7. Total harmonic distortion of the phase voltage.

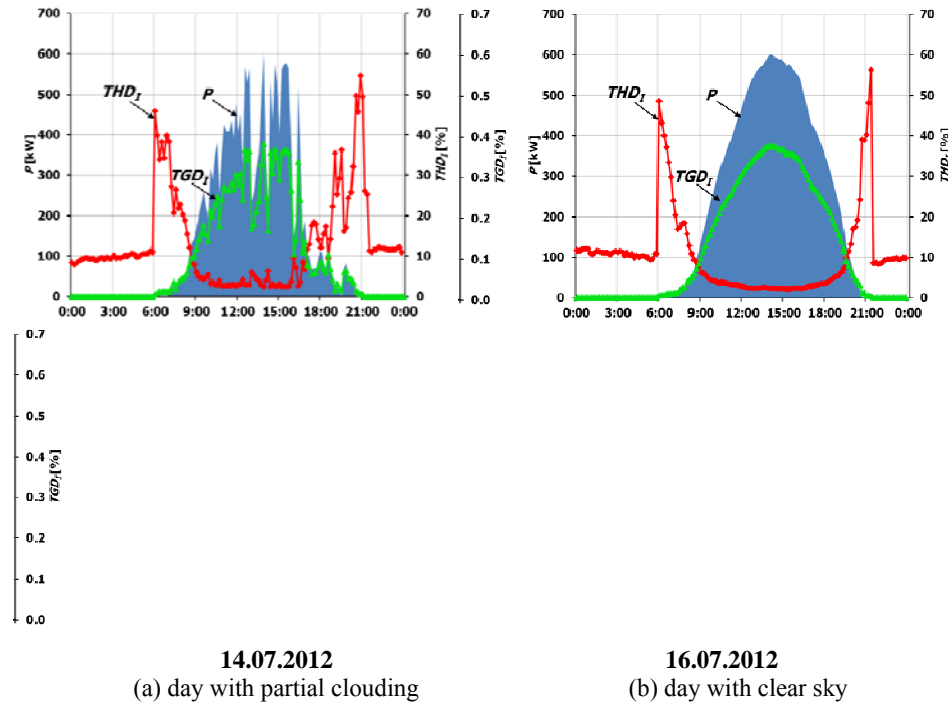


Fig. 8. Total harmonic distortion for the phase current.

In the analysis of the variation of the  $THD_I$  in Fig. 8 we must point out that, for installations with a high degree of variance, large  $THD_I$  values can lead to inadequate conclusions. To properly characterize the functioning of PV system from the standpoint of harmonic distortions produced in the PCC (*Point of Common Coupling*), we propose utilizing a new indicator value,  $TGD_I$  (*Total Generator Distortion*), specific to sources with a high degree of variance. The new value should be presented in relation with the nominal current ( $I_n$ ) given by the PV system:

$$TGD_I = \frac{\sqrt{\sum_{h=2}^{\infty} I_h^2}}{I_n}, \quad (1)$$

The relationship between the two values can be written as:

$$TGD_I = \frac{THD_I}{\sqrt{1+(THD_I)^2}} \cdot \frac{I}{I_n} \quad (2)$$

in which  $I$  is the value for the measured electric current.

Analyzing the data from Fig. 8 outlines the statement that the  $TGD_I$  indicator clearly defines the effect of harmonics in the electrical network through an accurate display of the transmitted power and the form of the voltage curve in the PCC, without relaying insignificant information in the reduced power generation time frame.

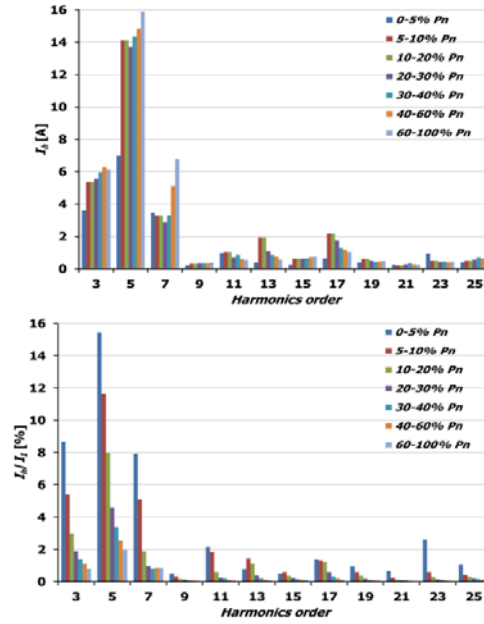
The previous aspects have been analyzed by carrying out a specific analysis of the individual harmonic distortion for the phase currents. In order to characterize the overall behaviour of the system, the study has been structured by partitioning the generation level into ranges having width expressed as per cent ranges of the rated power  $P_n$ , in particular identifying the ranges  $0 \div 5\% P_n$ ,  $0 \div 5\% P_n$ ,  $5 \div 10\% P_n$ ,  $10 \div 20\% P_n$ ,  $20 \div 30\% P_n$ ,  $30 \div 40\% P_n$ ,  $40 \div 60\% P_n$ , and  $60 \div 100\% P_n$ . Inside each range, a statistical analysis of the odd harmonic currents with harmonic order up to 50 has been made on the entire week, and the RMS harmonic current values corresponding to a non-exceeding probability of 90% have been identified. The rationale for using the 90% non-exceeding probability instead of the maximum value is to avoid to show results with high harmonic currents possibly depending on conditions with low probability of occurrence [15]. From the results, it appears that the most significant results can be seen for harmonic orders up to 25.

Fig. 9 shows that the RMS values of the harmonic currents exhibit relatively small variations for the same harmonic order when the generation level increases. The fifth harmonic component is the prevailing one. Individual harmonics at the third and seventh harmonic are also significant. The contribution at the other harmonic orders is less relevant. When the RMS values  $I_h$  are expressed in per cent with respect to the component  $I_1$  at the fundamental frequency, the reduction in the per cent values at the successive generation levels become apparent. This fact confirms that the low  $THD$  values at high generation levels are due to a reduced contribution of all the harmonic orders. The RMS values of the individual phase voltage harmonics are represented in Fig. 10. The fifth and seventh harmonic orders are the most relevant. The voltage values highly depend on the interaction of the PV system output with the other components connected to the grid. The voltage harmonics are at the same time cause and effect of the overall harmonic distortion in the system.

### 3.3. Considerations on the power factor

Fig. 11a shows the points representing the power factor in function of the generation level. The inverter control is set up in such a way to make the PV system working as close as possible to a resistive component. This behaviour is

basically confirmed when the PV system operates at generation levels above 30%. Conversely, when the generation level becomes relative low, the power factor goes down to low values [29]. However, as already remarked, the operation of the PV systems at low generation levels corresponds to low currents injected in the grid, whose effect is in any case poorly relevant to the system operation.



(a) RMS current values in ampere

(b) per cent values

Fig. 9. RMS and per cent values of the individual phase current harmonics (90% non-exceeding probability in one week) for different generation levels.

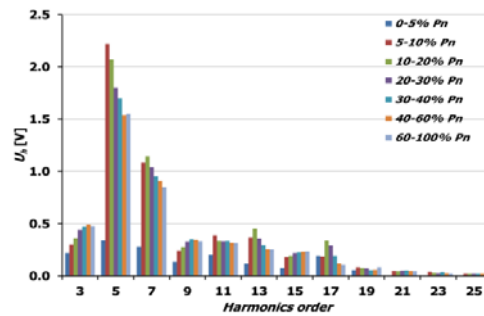
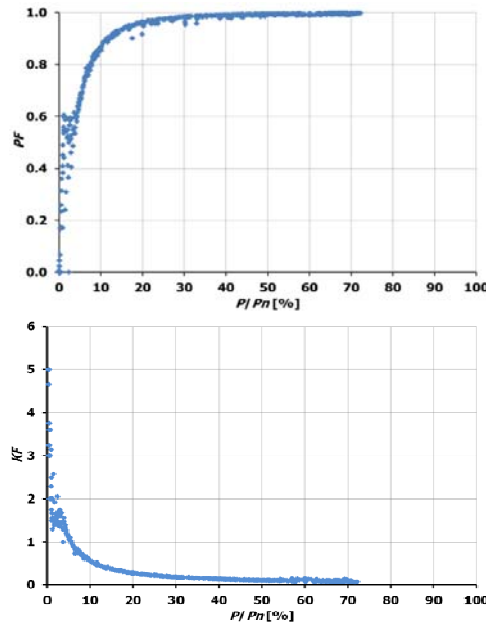


Fig. 10. RMS values of the individual phase voltage harmonics (90% non-exceeding probability in one week) for different generation levels.

In order to check whether the power factor values refer to positive or negative reactive power values, Fig. 11b shows the points representing the reactive factor  $KF$  values, where  $KF = (S^2 - P^2)^{(1/2)} / P$ , that is, the ratio between reactive and active power. It can be seen that the system always behaves with the same sign of the reactive power: in particular, the inverters behave as capacitors and the grid behaves as inductor. Even if the power factor is very close to unity when the power exceeds 50% of rated value, the reactive power is not completely negligible.



(a) power factor

(b) reactive factor

Fig. 11. Values of the power factor and reactive factor at the point of common coupling in the measurement period of one week, in function of the generation level.

#### 4. Conclusions

An experimental investigation of the harmonic distortion occurring at the point of common coupling of a number of PV inverters connected to the grid has been carried out on a PV plant of total rated power 834.5 kW. The measured data have been gathered from the installation through a network analyzer with high accuracy for a period of one week.

The analysis of the results show that the current harmonics generated by the PV system highly depend on the generation level. As such, conditions in which the solar irradiance is low or reduced by the effects of shadowing or

passing clouds lead to an increase of the harmonic distortion. However, this larger harmonic distortion is not harmful when the associated RMS value of the current is relatively low. In general, at high generation level the harmonic distortion is relatively low ( $<5\%$ ), and the inverter control operates in such a way that in the case analyzed the PV system is providing a positive contribution to the reduction of the distortion on the harmonic voltages with respect to the harmonic distortion occurring in the distribution system without the connection of the PV system.

## REFERENCES

- [1] European PV Industry Association, Global market outlook, online <http://files.epia.org/files/Global-Market-Outlook-2016.pdf>
- [2] F. Spertino, F. Corona, P. Di Leo, "Limits of Advisability for Master-Slave Configuration of DC-AC Converters in Photovoltaic Systems", IEEE Journal of Photovoltaics, in press, doi: 10.1109/JPHOTOV.2012.2203793.
- [3] DIN V VDE 0126-1-1:2006, "Automatic disconnection device between a generator and the public low-voltage grid", VDE-publisher, Berlin/Germany, Feb. 2006.
- [4] S. Islam, A. Woyte, R. Belmans, P.J.M. Heskes, P.M. Rooij, "Investigating performance, reliability and safety parameters of photovoltaic module inverters: test results and compliances with the standards", Renewable Energy, 31, 2006, 1157-1181.
- [5] Italian Electrotechnical Committee (CEI), "Tests for the verification of the functions of interface with the electrical network for the micro-generators", Italian Standard CEI 11-20, variant V2, 2007, Annex C.
- [6] Italian Electrotechnical Committee (CEI) "Electrical energy production system and uninterruptible power systems connected to I and II class network", Italian Standard CEI 11-20, variant V3, 2010.
- [7] A. Marinopoulos, F. Papandrea, M. Reza, S. Norrga, F. Spertino, R. Napoli, "Grid Integration Aspects of Large Solar PV Installations: LVRT Capability and Reactive power/Voltage support Requirements", Proc. IEEE PowerTech 2011, Trondheim, Norway, June 19-23, 2011, pp. 1-8.
- [8] Terna, "Regolazione tecnica dei requisiti di sistema della generazione distribuita" (in Italian), Annex A70, Technical Guide, 12/03/2012.
- [9] Autorità per l'Energia Elettrica e il Gas, "Interventi urgenti relativi agli impianti di produzione di energia elettrica, con particolare riferimento alla generazione distribuita, per garantire la sicurezza del sistema elettrico nazionale" (in Italian), Deliberazione 8 marzo 2012, 84/2012/r/eel.

- [10] A. Woyte, J. Nijs, R. Belmans, "Partial shadowing of photovoltaic arrays with different system configurations: literature review and field test results", *Solar Energy*, 74, 2003, 217-233.
- [11] D.G. Infield, P. Onions, A.D. Simmons, G.A. Smith, "Power quality from multiple grid-connected single-phase inverters", *IEEE Trans. Power Delivery*, 19 (4), 2004, 1983-1989.
- [12] M. Aiello, A. Cataliotti, S. Favuzza, G. Graditi, "Theoretical and experimental comparison of total harmonic distortion factors for the evaluation of harmonic and interharmonic pollution of grid-connected photovoltaic systems", *IEEE Trans. Power Delivery*, 21 (3), 2006, 1390-1397.
- [13] F. Batrinu, G. Chicco, J. Schlabbach, F. Spertino, "Impacts of grid-connected photovoltaic plant operation on the harmonic distortion", *Proc. IEEE Melecon 2006*, Benalmádena, Málaga, Spain, 16-19 May 2006, 861-864.
- [14] G. Chicco, J. Schlabbach, F. Spertino, "Performance of grid-connected photovoltaic systems in fixed and sun-tracking configurations", *Proc. IEEE PowerTech 2007*, Lausanne, Switzerland, 1-5 July 2007, paper no.388.
- [15] G. Chicco, J. Schlabbach and F. Spertino, "Experimental assessment of the waveform distortion in grid-connected photovoltaic installations", *Solar Energy*, 83 (7), 2009, 1026-1039.
- [16] M. Thomson, D.G. Infield, "Impact of widespread photovoltaic generation on distribution systems", *IET Renewable Power Generation*, 1 (1), 2007, 33-40.
- [17] J.H.R. Enslin, P.J.M. Heskes, "Harmonic interaction between a large number of distributed power inverters and the distribution network", *IEEE Trans. Power Electronics*, 19 (6), 2004, 1586-1593.
- [18] Canadian Solar components, web site <http://www.canadiansolar.com>.
- [19] L. Peng, L. Yaoyu, J.E. Seem, "Sequential ESC-Based Global MPPT Control for Photovoltaic Array With Variable Shading", *IEEE Trans. Sustainable Energy*, 2 (3), 2011, 348-358.
- [20] K. Ishaque, Z. Salam, M. Amjad, S. Mekhilef, "An Improved Particle Swarm Optimization (PSO)-Based MPPT for PV With Reduced Steady-State Oscillation", *IEEE Trans. Power Electronics*, 27 (8), 2012, 3627-3638.
- [21] A. Bidram, A. Davoudi, R.S. Balog, "Control and Circuit Techniques to Mitigate Partial Shading Effects in Photovoltaic Arrays", *IEEE Journal of Photovoltaics*, 2012, in press.
- [22] IMT Solar components, web site <http://www.imtsolar.com>.
- [23] G. Chicco, J. Schlabbach, F. Spertino, "Characterisation and assessment of the harmonic emission of grid-connected photovoltaic plants", *Proc. IEEE Power Tech 2005*, St. Petersburg, Russia, 27-30 June, 2005, paper no.66.
- [24] CENELEC (European Committee for Electrotechnical Standardisation), "Voltage characteristics of electricity supplied by public distribution systems", *European Norm EN 50160*, 2011.
- [25] Italian Electrotechnical Committee (CEI), "Sistemi fotovoltaici (FV) - Caratteristiche dell'interfaccia di raccordo con la rete", *Standard CEI EN 61727 (CEI 82-9)*, 2007.
- [26] International Electrotechnical Commission (IEC), "Testing and measurement techniques – Part 4-7: General guide on harmonics and interharmonics measurement and instrumentation for power supply systems and equipment connected thereto", *IEC Std. 61000-4-7*, 2002.
- [27] International Electrotechnical Commission (IEC), "Electromagnetic compatibility (EMC) Part 3-2: Limits for harmonic current emission (equipment input current  $\leq 16$  A per phase)", *IEC Std. 61000-3-2*, 2000.
- [28] International Electrotechnical Commission (IEC), "Electromagnetic compatibility (EMC) Part 3-12: Limits for harmonic currents produced by equipment connected to public low-voltage systems with input current  $< 75$  A per phase", 2003.



- [29] G. Chicco, R. Napoli, F. Spertino, "Experimental evaluation of the performance of grid-connected photovoltaic systems", Proc. IEEE Melecon 2004, Dubrovnik, Croatia, 3, 1011-1016.